FULL PAPER

Characteristics and longitudinal extent of VLF quasi-periodic emissions using multi-point ground-based observations

Claudia Martinez-Calderon[1]* , Tomoka Oonishi[1], Kazuo Shiokawa[1], Jyrki K. Manninen[2], Alexey Oinats[3] and Mitsunori Ozaki[4]

Abstract

Quasi-periodic (QP) emissions are a type of magnetospheric ELF/VLF waves characterized by a periodic intensity modulation ranging from tens of seconds to several minutes. Here, we present 63 QP events observed between January 2017 and December 2018. Initially detected at the VLF receiver in Kannuslehto, Finland (KAN, MLAT$=67.7°$N, $L=5.5$), we proceeded to check whether these events were simultaneously observed at other subauroral receivers. To do so we used the following PWING stations: Athabasca (ATH, MLAT$=61.2°$N, $L=4.3$, Canada), Gakona (GAK, MLAT$=63.6°$N, $L=4.9$, Alaska), Husafell (HUS, MLAT$=64.9°$N, $L=5.6$, Iceland), Istok (IST, MLAT$=60.6°$N, $L=6.0$, Russia), Kapuskasing (KAP, MLAT$=58.7°$N, $L=3.8$, Canada), Maimaga (MAM, MLAT$=58.0°$N, $L=3.6$, Russia), and Nain (NAI, MLAT$=65.8°$N, $L=5.0$, Canada). We found that: (1) QP emissions detected at KAN had a relatively longer observation time (1–10 h) than other stations, (2) 11.3% of the emissions at KAN were observed showing one-to-one correspondence at IST, and (3) no station other than IST simultaneously observed the same QP emission as KAN. Since KAN and IST are longitudinally separated by 60.6°, we estimate that the maximum meridional spread of conjugated QP emissions should be close to 60° or 4 MLT. Comparison with geomagnetic data shows half of the events are categorized as type II, while the rest are mixed (type I and II). This study is the first to clarify the longitudinal spread of QP waves observed on the ground by analyzing simultaneous observations over 2 years using multiple ground stations.

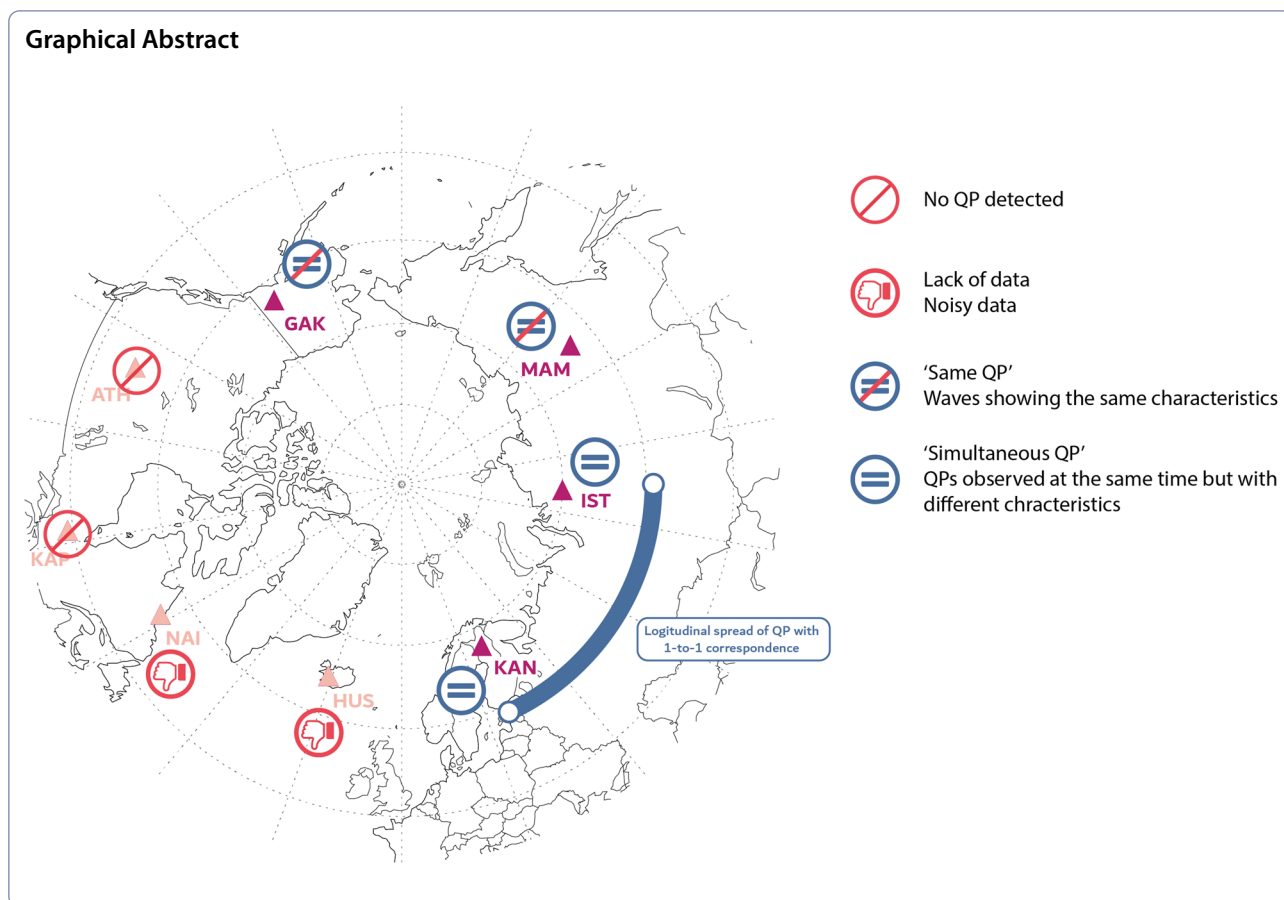**Keywords** VLF waves, Quasi-periodic emissions, Ground-based stations, Conjugated events

*Correspondence:
Claudia Martinez-Calderon
claudia@isee.nagoya-u.ac.jp
Full list of author information is available at the end of the article

Martinez-Calderon *et al. Earth, Planets and Space*   (2023) 75:148

Page 2 of 13

Graphical Abstract

Introduction

Very low frequency (VLF) emissions are natural waves of magnetospheric origin propagating in the whistler-mode and observed in the frequency range between 3 and 30 kHz (Barr et al. 2000). They are usually generated near the geomagnetic equator as a consequence of resonant cyclotron interactions with radiation belt electrons having energies of hundreds of keV. The study of VLF waves is of particular importance as through wave–particle interactions they can accelerate or scatter electrons, and thus play a fundamental role in radiation belt dynamics (e.g., Hayosh et al. 2013; Horne et al. 2005; Meredith et al. 2003; Thorne 2010). Quasi-periodic (QP) emissions are a type of VLF wave characterized by a periodic modulation of wave intensity with typical periods of tens of seconds up to several minutes. QP emissions have also historically been classified into two types depending on whether they are (type I) or not (type II) detected along geomagnetic pulsations of the same period (e.g., Kitamura et al. 1968; Sato and Fukunishi 1981; Sato et al. 1974). While both types of QP emissions are believed to be related to cyclotron instabilities, type I emissions would be modulated by geomagnetic pulsations (Nemec et al. 2013a, b;

Kimura 1974; Sato and Fukunishi 1981; Sato and Matsudo 1986), while type II emissions are to be directly related to auto-oscillations of cyclotron instability of the radiation belts (Trakhtengerts & Rycroft 2008; Manninen et al. 2013, 2014). However, some studies have shown that the separation between these two categories is not as clear as previously believed, particularly when using satellite observations, and that both types could have the same generation mechanisms (Tixier and Cornilleau-Wehrlin 1986; Sato and Matsudo 1986; Nemec et al. 2013a, b; Hayosh et al. 2013).

QP emissions can resonantly interact with energetic electrons and cause electrons to precipitate with the same periodicity (Hayosh et al. 2014), and, therefore, play a part in the regulation of radiation belt dynamics. Especially, because these types of waves are known to spread considerably across L-shells (Nemec et al. 2018; Titova et al. 2015). Still, the longitudinal spread of QP emissions has rarely been studied because there are only a few examples of events observed simultaneously at multiple locations.

From observations in the inner magnetosphere, Martinez-Calderon et al. (2020) studied a QP event

Martinez-Calderon *et al. Earth, Planets and Space* (2023) 75:148

Page 3 of 13

simultaneously observed by three satellites (Arase and the Van Allen probes). This event showed one-to-one correspondence of QP elements at all locations, meaning the waves detected by the three satellites were the same or coming from the same source region. From these observations, they calculated that the area of space where the QP emissions showed one-to-one correspondence was at least 1.21 R_E radially and 2.26 in MLT, suggesting an azimuthally distributed source. This same QP event was also partially detected by a ground station in Russia, showing in some cases one-to-one correspondence. Comparing the observations in space and on the ground, they found that temporal changes in spectral features pointed to either a global source region with smaller sources showing different properties or to multiple sources with an external mechanism behind the changes in features. Multi-point observations such as the study described above can yield significant information on the properties of QP emissions; however, such a type of comparative study has not been performed based on ground data better suited to elucidate the longitudinal extent of the waves. Yonezu et al. (2017) investigated the occurrence of simultaneous ELF/VLF waves at subauroral and auroral latitudes and found that the simultaneous occurrence rates decreased with the MLT separation between two stations. Takeshita et al. (2019) analyzed the longitudinal spread of a variety of magnetospheric ELF/VLF waves from data obtained over 2 months at six ground stations at subauroral latitudes. In addition, in a further study, Takeshita et al. (2020) estimated the longitudinal extent of the source region of ELF/VLF waves associated with substorm injections and eastward electron drift. However, none of these previous studies distinguished among all the wave types observed (e.g., chorus, QP, hiss) nor did they focus on studying the properties and longitudinal extent of each type of wave separately. In addition, they did not take into account the one-to-one correspondence of waves at multiple locations to determine if the waves were the same or coming from the same source region.

Therefore, this paper will be the first one to use multiple ground stations at similar latitudes to specifically investigate the extent of QP emissions as seen from the ground. We will use QP waves simultaneously observed at multiple stations showing the same spectral and temporal features to elucidate the longitudinal spread of QP waves showing one-to-one correspondence. We start from a list of QP emissions detected at Kannuslehto, Finland (KAN, MLAT = 67.7°N, $L = 5.5$), and then we compare it to data from the other seven PWING stations to determine if the same emissions (or from the same source) are observed simultaneously. We will discuss the

conditions of observation, and additional geomagnetic data will be examined to determine the QP type of the waves.

Data set

The PWING network consists of eight ground stations approximately located at 60 degrees (corresponding to $L \sim 4$) of magnetic latitude (MLAT), thus encircling the Earth like a crown as shown in Fig. 1. The PWING acronym stands for "study of dynamical variations of Particles and Waves in the INner magnetosphere using ground-based network observations". These ground stations are continuously measuring the global conditions of waves and particles thanks to all-sky and auroral cameras, VLF loop antennas, induction magnetometers, and riometers. More details on the entire PWING network can be found in Shiokawa et al. (2017).

In this study, we will specifically use data from the PWING VLF receivers that measure wave magnetic field
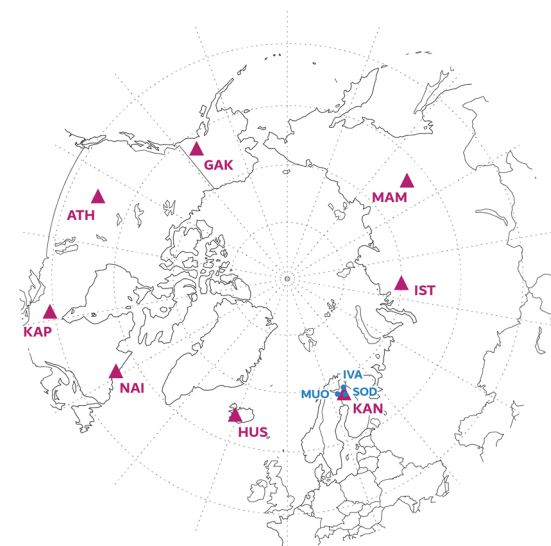
	Station	Name	Geographic latitude	Geographic longitude	Geomagnetic latitude	Geomagnetic longitude	L-shell
VLF	Athabasca	ATH	54.6°N	246.4°E	61.1°N	52.0°W	4.5
	Gakona	GAK	62.4°N	214.8°E	63.6°N	91.2°W	4.9
	Husafell	HUS	64.7°N	339.0°E	69.2°N	71.5°E	5.5
	Istok	IST	70.0°N	88.0°E	60.7°N	166.5°E	6.1
	Kannuslehto	KAN	67.7°N	26.3°E	64.4°N	119.4°E	5.4
	Kapuskasing	KAP	49.4°N	277.8°E	58.6°N	12.0°W	3.7
	Maimaga	MAM	63.1°N	129.6°E	53.9°N	163.0°W	3.6
	Nain	NAI	56.5°N	298.3°E	65.7°N	14.8°W	4.9
MAG	Ivalo	IVA	68.6°N	27.3°E	65.1°N	108.6°E	5.9
	Muonio	MUO	68.0°N	23.5°E	64.7°N	105.2°E	5.7
	Sodankyla	SOD	67.4°N	26.6°E	63.9°N	107.3°E	5.4

Fig. 1 VLF receivers and magnetometer locations. Locations of all the VLF receivers (magenta triangles) and the magnetometers (blue circles) used in this study. Top shows the location of the stations in geographic coordinates, and bottom gives the geographic and geomagnetic coordinates of the stations, as well as the L-shells of the VLF receivers (using IGRF-13)

variations in the north–south and east–west directions using two distinct loop antennas with a sampling rate of 40 kHz (Martinez-Calderon 2016; Shiokawa et al. 2017). We note that the KAN receiver in northern Finland has a different build and configuration, with a sampling frequency of 78.125 kHz and a sensitivity of 0.088 fT, making it the most sensitive in the world. Further details can be found in Manninen (2005). We also note that for ground observations, wave-normal vectors of downgoing VLF whistler-mode waves should lie within a transmission cone angle given by a relative index of whistler mode waves and Snell's law (e.g., Ozaki et al. 2008, 2010).

To determine if QP emissions are type I or II we used data from IMAGE magnetometers nearby KAN. The IMAGE network consists of 47 magnetometer stations in multiple European countries by institutes from Finland, Germany, Norway, Poland, Russia, Sweden, Denmark, and Iceland (Tanskanen 2009). Here we only use data from Ivalo (IVA), Muonio (MUO), and Sodankylä (SOD), which are close in latitude and longitude to KAN. In some cases, we also used data from the pulsation magnetometers at the same locations.

Event selection

In this study, we use KAN as the starting station or station of reference. We chose this considering three factors: first, KAN is the most sensitive station in the PWING network. Second, it is the only station where a system filtering out sferics is implemented, making it easier for us to distinguish the waves from background noise. Finally, it appears to have the highest occurrence rate (~ 32%) for all types of ELF/VLF emissions among all PWING stations (Takeshita et al. 2019).

We started by analyzing VLF observations between January 2017 and December 2018 to find the timings in which KAN detected QP emissions. A single event is defined as continuous observations of waves without interruptions longer than their perceived periodicity. If two or more QP events are observed at different times of the day they are considered separate events. In addition, if multiple QP emissions are simultaneously observed at different frequencies but at the same timings, they will also be considered as a single event. We note that KAN does not operate continuously but on a campaign basis, usually turning off the receiver yearly during the arctic summer, typically from May to August. Therefore, during the 2-year study period, we actually have approximately 19 months of possible observations barring any difficulties with the equipment. We calculated that for the 19-month period in question, KAN data were available for 10,624 h out of a total possible of 10,910 h, meaning a coverage of 97.38%. In this time frame, KAN detected 44 QP events of various duration, the shortest being 30 min

and the longest approximately 10 h. The sum of all these events is a total of 9190 min or about 153 h of observations. This means that the global occurrence rate of QP emissions at KAN during this period was ~ 1.45%.

From the previously mentioned list of 44 events, we proceeded to identify whether QP waves were observed at the same date and timings at the other PWING stations (Fig. 1) by plotting the hourly wave spectra. An example of such 1-h plots is shown in Fig. 2, where we compare the power spectrum density observed at KAN (top) and IST (bottom) on 21 December 2017 from 19:00 to 20:00 UT. In this case, the two stations simultaneously detected a QP emission centered around 2 kHz with a period of about 2–3 min. In particular, after approximately 19:25 UT, we note that both locations show one-to-one correspondence of QP elements between KAN and IST. Black and white arrows in Fig. 2a, b, respectively, make this correspondence easier to visualize. This specific property will be discussed in detail in later sections of this paper. To facilitate a comparison of all the data we have rounded up the start and end timings of the events to the closest 5-min mark that includes the event. For the example shown in Fig. 2, the period showing the same waves will be considered as 19:25 to 19:50 UT.

As such, we proceeded to compare all 44 events detected at KAN and the spectra in all other PWING stations. If QP waves were observed at any other station we noted their location, frequency, period, and intensity. We found a total of 22 of these events and separated them into two categories. The first group corresponds to simultaneous observations of QP emissions at multiple locations but without any common features. The second group corresponds to those events which show the same spectral and timing features in multiple locations, and show one-to-one correspondence of QP elements. Their specific features will be discussed in detail in the next section.

Event analysis

Group 1: simultaneous QPs

As described in Sect. "Event selection", Group 1 corresponds to simultaneous observations of QP emissions at multiple locations but without any common features. This means that although waves are observed simultaneously, they are detected at different frequencies or show different periodicity and other features. This group will be known as 'simultaneous QPs' events.

Figure 3 shows the power spectrum density observed at KAN (top) and IST (bottom) on 31 January 2018 from 02:30 to 02:40 UT. Using KAN as a reference, we note that the QP emission detected at IST has different physical characteristics than the one observed at KAN. The waves at KAN are detected between 2.3 and 3.3 kHz and
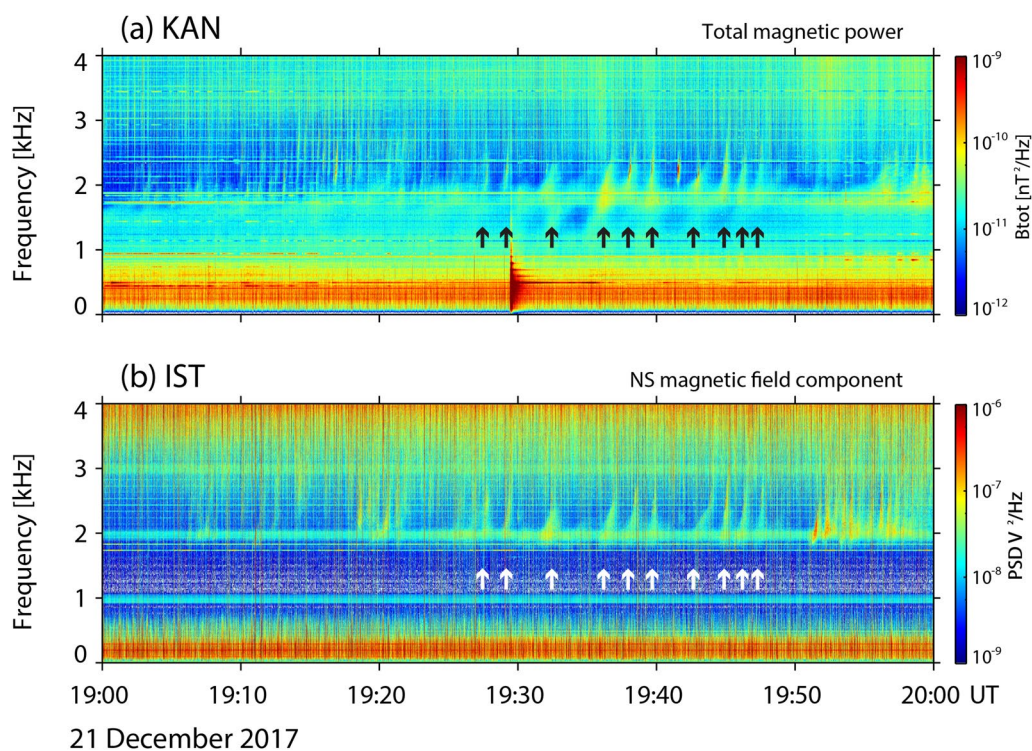
Fig. 2 1-h plot wave spectra on 21 December 2017. Example of 1-h plot wave spectra on 21 December 2017 from 19:00 to 20:00 UT showing a QP emission detected at two locations: **a** KAN and **b** IST. In this particular case, the QP emission shows one-to-one correspondence of elements as indicated by the black and white arrows, respectively
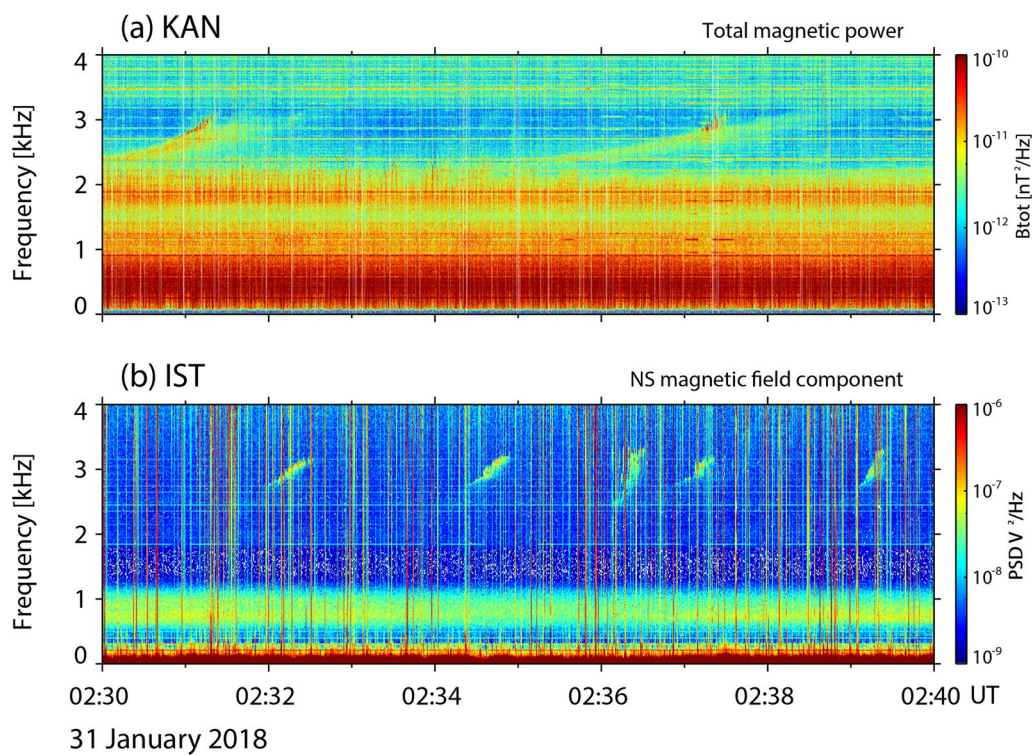

Fig. 3 10-min plot wave spectra on 31 January 2018. Wave spectra at **a** KAN and **b** IST detected on 31 January 2018 from 02:30 to 02:40 UT showing two QP emissions with different properties at the two locations. This event corresponds to the 'simultaneous QP' group

Martinez-Calderon *et al. Earth, Planets and Space*   (2023) 75:148

Page 6 of 13

have a periodicity of about 6 min, with each QP element lasting about 4 min. On the other hand, the QP emission at IST has a much higher frequency, in the range of 2.7–3.2 kHz, much shorter elements (∼ 30 s), and a periodicity of 2.5 min (the burst at ∼ 02:36 UT showing slightly different features seems to be unrelated). Since the QP features are different at different stations, we consider these events as 'simultaneous QPs'. We detected a total of 10 events of this type: 1 at MAM, 2 at GAK, and 6 at IST. All events combined lasted 1020 min or 17 h, corresponding to ∼ 11.1% of all QP observations at KAN.

While spectral features of the waves could be affected by an external pulsation mechanism or be subject to some dispersion during their propagation, these do not account for the very distinct spectral shapes observed at both locations in cases such as those of Fig. 3. We also note that, in theory, the frequency of the waves should not change during their propagation from their source region in the magnetosphere until their detection on the ground. This suggests that if we are observing waves with different frequencies, they should not come from the same source region. However, a source can emit over a wide range of frequencies, meaning those frequencies could reach different points due to their specific propagation path within the magnetosphere. This means that if the waves have different frequencies, we would be unable to tell if they come from the same source region. Therefore, in this study, we will consider only waves that show the same frequencies or frequency variations as those coming from the same source region. Therefore, 'simultaneous QPs' observed at multiple stations are assumed as coming from different source regions in the magnetosphere, and even though they are detected at the same time they are not necessarily related to each other.

We do note that all the stations where these events are detected are located eastward of KAN, our station of reference (Fig. 1). We could not find a specific reason why waves would only be detected to the east of a particular location, as even if electrons drift eastward, most of the events are detectedwhile the stations are on the dayside and, therefore, should not be strongly influenced by eventual injections from midnight. We also should point out that the station with the highest 'simultaneous QPs' is IST, which is the closest station to the east of KAN. The easiest assumption would be that in most cases the source region is likely located closer to either of these stations or in between them, making it harder for the waves to reach stations further apart. As we have fewer cases where waves were detected by MAM and GAK, we could also suppose that there is a much larger source region located somewhere between KAN and GAK but the waves are more likely to reach KAN and IST due to propagation factors, either in the magnetosphere or

ionosphere. Meaning, for example, that it could be harder for the waves to cross the ionosphere near MAM or GAK, or that there is easier ducting nearby KAN and IST.

Group 2: same QPs

The second group of events is the one in which we have the most interest. These are cases that show the same spectral and timing features at multiple locations and show clear one-to-one correspondence of QP elements, as shown in Fig. 2. As these waves show the same temporal and spectral characteristics, we can assume that they are either the same waves or they are being generated by the same source region. This group will be referred to as 'same QPs' and will allow us to identify the longitudinal extent of the QP emissions detected by the PWING stations.

Figure 4 illustrates this group using a close-up version of Fig. 2. It shows the spectra detected at KAN (top) and IST (bottom) on 21 December 2017 between 19:30 and 19:40 UT. Again, using KAN as a reference, we note that besides some scattering in the spectra that can be due to the propagation through the ionosphere, both emissions show the same frequency (∼ 1.8–2.5 kHz), the same periodicity (4 then 2 min), same shape, and timings. We can easily see the one-to-one correspondence of four QP elements, each with a durations of about 1 min. We also note the same smaller vertical elements within the first single element starting at ∼ 19:31 UT indicated by the black arrows in both panels. These types of vertical structures are also observed at the top right of the third and fourth QP elements. However, it is not as clearly seen as for the first element as the sferics make them hard to make out at IST. Nonetheless, these features make it easier for us to determine that these waves are at least coming from the same source region.

We found 13 events in the 'same QPs' category, and contrary to the previous group, they were only detected between KAN and another station: IST. Table 1 shows the details of all the 'same QPs' events. For each event, we note the date of observation, starting time and ending time at each station, and finally the start and end of the one-to-one correspondence between the two stations. We have also included the frequency range of the emissions and their perceived periodicity during the times when they were detected at the two locations. While not included in the table to avoid over-cluttering, we also estimated the intensity of the emissions. This means that we noted the frequencies, where the emission was stronger and estimated the overall intensity by eye and noted those values. We found that in half of the cases, both ground stations detected the 'same QPs' with similar intensities, meaning in the same order of magnitude. In three cases, both emissions showed
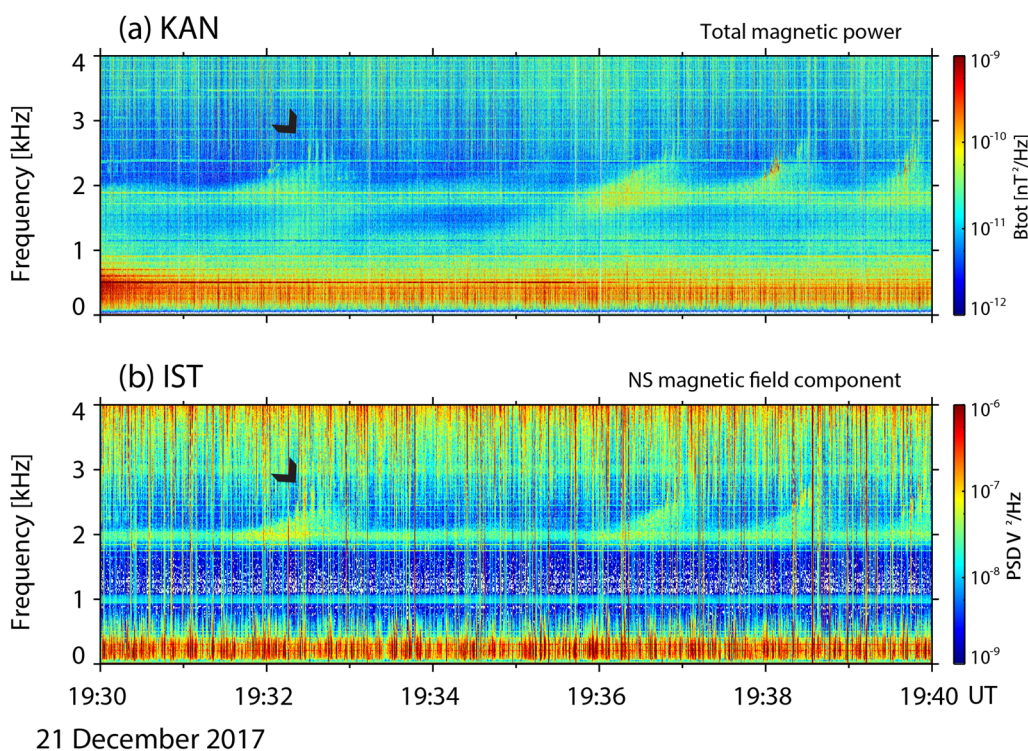
Fig. 4 10-min plot wave spectra on 21 December 2017. Wave spectra at (top) KAN and (bottom) IST detected on 21 December 2017 from 19:30 to 19:40 UT showing two QP emissions with one-to-one correspondence at the two locations

Table 1 Table of the 13 events of 'same QPs' events

DATE	KAN Total QP observation			IST Total QP observation			'Same QP' observation				
	Start [UT]	End [UT]	Minutes	Start [UT]	End [UT]	Minutes	Start [UT]	End [UT]	Minutes	Freq. range [kHZ]	Period [s]
2017-11-14	06:05	09:30	205	05:20	09:20	240	06:05	08:55	170	1.5 – 4.5	20 – 40
2017-11-20	01:40	08:05	385	01:30	03:35	125	01:35	02:45	70	1.7 – 3.2	40 – 50
	08:45	09:25	40	08:50	11:05	135	08:55	09:25	30	0.7 – 1.5	3
	09:40	15:00	320	14:00	14:50	50	14:10	14:25	15	2.0 – 4.8	25
2017-12-08	10:05	11:00	55	10:05	10:50	45	10:05	10:50	45	0.5 – 2.0	30 – 60
2017-12-21	19:00	23:50	290	19:20	20:15	55	19:25	19:50	25	1.6 – 2.5	120 – 240
2017-12-26	09:10	13:55	285	05:45	09:54	249	09:10	09:55	45	0.4 – 1.6	15 – 20
				10:15	10:35	20	10:15	10:35	20	0.5 – 1.5	30
2017-12-29	04:00	05:55	345	00:10	06:40	390	04:00	05:55	115	2.0 – 2.9	30
	06:55	09:10	135	06:50	10:30	220	06:55	09:10	135	1.4 – 2.8	20 – 40
	13:20	17:10	230	10:55	15:15	260	13:20	15:00	100	1.7 – 3.0	15 – 20
2017-12-30	02:35	05:40	185	02:35	04:00	85	02:40	03:20	40	1.8 – 3.2	40
2018-11-19	05:00	07:50	170	04:20	07:30	190	05:00	07:30	150	3.2 – 4.6	240 - 360

Table showing the 13 events of 'same QPs' observed at KAN and IST. For each event, we note the date, the starting and ending time at KAN and IST, respectively, and the timings, where both stations see the same QP emissions. We also note the frequency range and periodicity of the QP emissions during the timings of 'same QPs' detection

intensities in the 10^{-11} [nT^2/Hz] range, and in four cases 10^{-10} [nT^2/Hz]. The other half of the cases showed, on average, an intensity difference of one order of

magnitude between KAN and IST (the maximum being two orders of magnitude, between 10^{-10} and 10^{-12} [nT^2/ Hz]). We note that at IST, 10^{-6} [V^2/Hz] approximately

Martinez-Calderon *et al. Earth, Planets and Space*   (2023) 75:148

Page 8 of 13

corresponds to 10^{-11} [nT^2/Hz] and the plots shown here are made with uncalibrated data for better visualization. Having such similar intensities means that it is very likely that the source region was close to the stations, further supporting the findings of Martinez-Calderon et al. 2020 of a longitudinally distributed source region. However, this could also be the result of ducted propagation from the source to the two receivers.

We should mention that if the waves are detected by the receiver as coming directly from the ionosphere, they show right-handed polarization. If the waves bounced back at least once in the Earth-ionosphere waveguide, then they would be detected by the receiver on the ground as left-hand polarized (Ozaki et al. 2010). From KAN data, we found that a majority of the cases were strongly right-handed polarized, with one showing left-hand polarization and two cases showing mixed values. Unfortunately, polarization analysis from IST is not currently available due to the noise levels at the station. In addition, if the waves had bounced back in the waveguide then we would expect a significant loss of intensity. Particularly, since the distance between the two stations is approximately 2400 km. As most cases show similar intensities at IST and KAN, added to the previous point, we do not believe that these cases had significant spatial spread due to propagation in the waveguide.

The duration of the 'same QPs' events at both locations was a combined total of 960 min or 16 h, corresponding to ∼10.4% of the total QP observation time at KAN. This is a similar occurrence rate to that of the group of 'simultaneous QPs', meaning that observing the 'same QP' at IST has about the same chance as both stations detecting an unrelated emission.

We also note that the total duration of each QP event was different between KAN and IST. At IST, the events lasted for approximately 34.4 h, while at KAN, their overall duration was 44 h. The difference between these two numbers could be related to the difficulty of waves propagating to IST; however, it can also be partially explained by our inability to accurately detect features at the much noisier station of IST. This problem could be tackled by trying to integrate a sferics filter similar to the one used in KAN to reduce noise levels. We could also consider focusing on high-intensity events at KAN as a starting point to see how far these events can be detected by other PWING stations or, consider another station as a reference instead of KAN. Data from the newly installed (operational since October 2022) Oulujarvi VLF receiver approximately 370 km south of KAN and in similar longitudes could also be included. However, all these considerations are outside of the scope of this paper and should be taken into account for further study on the upper estimates of the azimuthal extent of the waves.

Longitudinal extent of QP emissions

As discussed in Sect. "Group 2: same QPs", the events where KAN and IST show one-to-one correspondence of QP waves amount to ∼10% of the total QP observation time at KAN. This result suggests that if we consider only the same QP waves or those emissions from the same source region, then the large majority of these (90%) detected at KAN cannot reach IST. The distance between KAN and IST is approximately 62° in the longitudinal direction, thus suggesting a large majority of emissions from the 'same QPs' group have a longitudinal extent of less than 4 MLT. For the remaining 10% of 'same QPs' detected at KAN that managed to reach IST, none was observed at the next station of MAM. KAN and MAM being ∼104° apart, we can estimate that even in the best-case scenario, QP emissions showing one-to-one correspondence can only extend to distances shorter than 7 MLT.

However, it is also important to note that the VLF receiver of HUS, closest to KAN to the west, is significantly noisier than the rest of the PWING stations. HUS is surrounded by sheep and a vast electric fence to keep them in place, which is the likely source of the noise seen at the station. It is entirely possible that the detection of 'similar QPs' emissions to those in KAN was affected by our inability to distinguish the emissions from the background noise. In addition, the second most westward station from KAN, NAI, has almost no data available as it is run by a generator and thus has no automatic continuous observations. It is possible that because of the noise and lack of data to analyze at both HUS and NAI, we are missing the westward extension of the 'same QPs'. All the same, we did not detect any one-to-one correspondence between QP waves from KAN and KAP, the third station to the west of KAN. This means that even if we missed detecting QP emissions at NAI or HUS these were still unable to reach KAP. The distance between KAN and KAP is ∼108°, corresponding to a distance of 7.2 MLT. This is a very close value to the one found when considering the eastward spread of 'similar QPs'. From this, we can conclude that, in either case, the maximum longitudinal extension of QP emissions showing one-to-one correspondence should not be greater than 7 MLT.

In addition, Takeshita et al. (2019) found a clear relationship between the total occurrence probability of ELF/VLF waves and the longitudinal distribution of the magnetic field intensity in the ionosphere. They concluded that waves are less likely to be generated at the longitudes of both hemispheres with weaker ionospheric magnetic field intensity due to the loss of high-energy electrons. These electrons who are responsible for generating the waves in the magnetosphere become lost to the ionosphere in the areaswhere the ionospheric magnetic field

Martinez-Calderon *et al. Earth, Planets and Space*   (2023) 75:148

Page 9 of 13

intensity is weaker. The two stations with the highest magnetic field are KAN followed by IST. This means that it is possible that QP emissions are being generated at higher rates and closer to KAN and IST as their magnetic field strength is larger than that at other stations. Assuming a source region in between the stations, it is more likely for the waves from the same source to be detected at these locations.

Takeshita et al. (2019) also found that, in general, all ELF/VLF wave activity is very likely to cover about 76° longitudinally, corresponding to approximately 5 MLT. Similarly, Takeshita et al. (2020) found that a wave, possibly driven by magnetospheric compression by the solar wind, had a minimum longitudinal extent of 5 MLT. Our results found that the longitudinal extent of a large majority of 'same QPs' was slightly shorter at about 4 MLT. These results are consistent as neither of these studies considered separation by emission type; therefore, it seems natural that values considering only QP emissions would be narrower than those including all other ELF/VLF emissions. In addition, they also did not take into account one-to-one correspondence between emissions at multiple locations as we have done here. On the other hand, Martinez-Calderon et al. (2020) did study a QP event that showed one-to-one correspondence between three satellites in the inner magnetosphere. They found that the longitudinal spread of the area of one-to-one correspondence was about 2.26 MLT or about half the distance found in this study. Nemec et al. (2018) analyzed QP events observed during the first 5 years of the Van Allen Probes spacecraft, mostly near the equatorial region believed to be the source of the events. Using data from the two spacecraft, they determined that the spatial extent of the emissions was typically ~ 1 R_E in radial distance and 1.5 h in MLT. However, both these results were obtained in space and much closer to the source region of QP waves. More recently, Bezdekova et al. (2020) made the analysis of simultaneous measurements of QP emissions between the same data set used by Nemec et al. (2018) and KAN. From 26 conjugated events, they found that the spatial extent of the emissions was typically within 40° of geomagnetic longitude, also slightly smaller than the values found in this study.

We also note that, independently of their propagation mode (ducted or unducted), while the waves can fan outward in latitude during propagation, their longitudinal extent should not be too large as to encompass multiple MLT hours. Backward ray tracing has shown that the rays for whistler-mode chorus at low altitudes concentrate in the local meridian for waves with frequencies below 820 Hz, at L-shells in the range of 3.65–7.61 (Santolik et al. 2006). Another study made by Parrot et al. (2003) using 3D ray tracing on chorus waves at selected

frequencies below 912 Hz found similar results, meaning that this longitudinal spread reflects a good approximation of the actual size of the source region. This would suggest then that the size of the source region of QP waves can be up to 4 MLT. As there are not that many 3D ray tracing studies that focus on this particular property of chorus and whistler-mode waves, we also note that in the case of equatorial noise, small deviations in the azimuth of the wave vector can result in a significant spread in MLT (up to 0.5 R_E) for frequencies of 100 Hz to 1 kHz (Santolik et al. 2016). As equatorial noise propagates toward the Earth, the wave frequency starts to be below lower hybrid frequency and then it is the same mode as chorus. Therefore, detailed 3D ray tracing should be considered to address these questions properly and specifically for QP emissions, and should be the subject of further studies.

To get more information on wave propagation we compared the timings of detection of the 'same QPs' events at KAN and IST. To do so we calculated the correlation coefficient of the events between the minimum and maximum frequency detected (every 100 Hz) and with appropriate timing windows for each case, to find the best possible correlation. Once this was determined, we calculated the cross-correlation coefficient to check the times where the correlation is the highest. However, due to noise at IST, overlapping waves and/or weaker power of the emission compared to the background, we did not find adequate results for all cases. Only 4 out of the 13 cases yielded significant results. We found that for these cases the maximum correlation was between 0.30 and 0.47, with a timing difference between the stations of 1.25 s to 2.49 s. Even though the correlation coefficients are moderate (probably due to the noise at IST) these results suggest that it is likely the waves reached one ground station first, and then the second one after a single or even double magnetospheric reflection. As the waves show similar intensities, it is very likely that they could have been ducted to both stations. Unfortunately none of the cases were detected by any spacecraft in the magnetosphere, besides one of the cases (26 December 2017 at 10UT) that has already been discussed in Martinez-Calderon et al. (2021).

Finally, we need to consider that we are using KAN as our reference point, and therefore, the comparison with the other stations could be biased. Meaning that if we did the same study using another PWING station as a reference the results could be different. However, as KAN is the station with the clearest spectrograms and the highest expected occurrence rate, we anticipated that it would be the one to give us the best results. Another point to consider is that during the period of this study, KAN was not active during the arctic summer, meaning that we
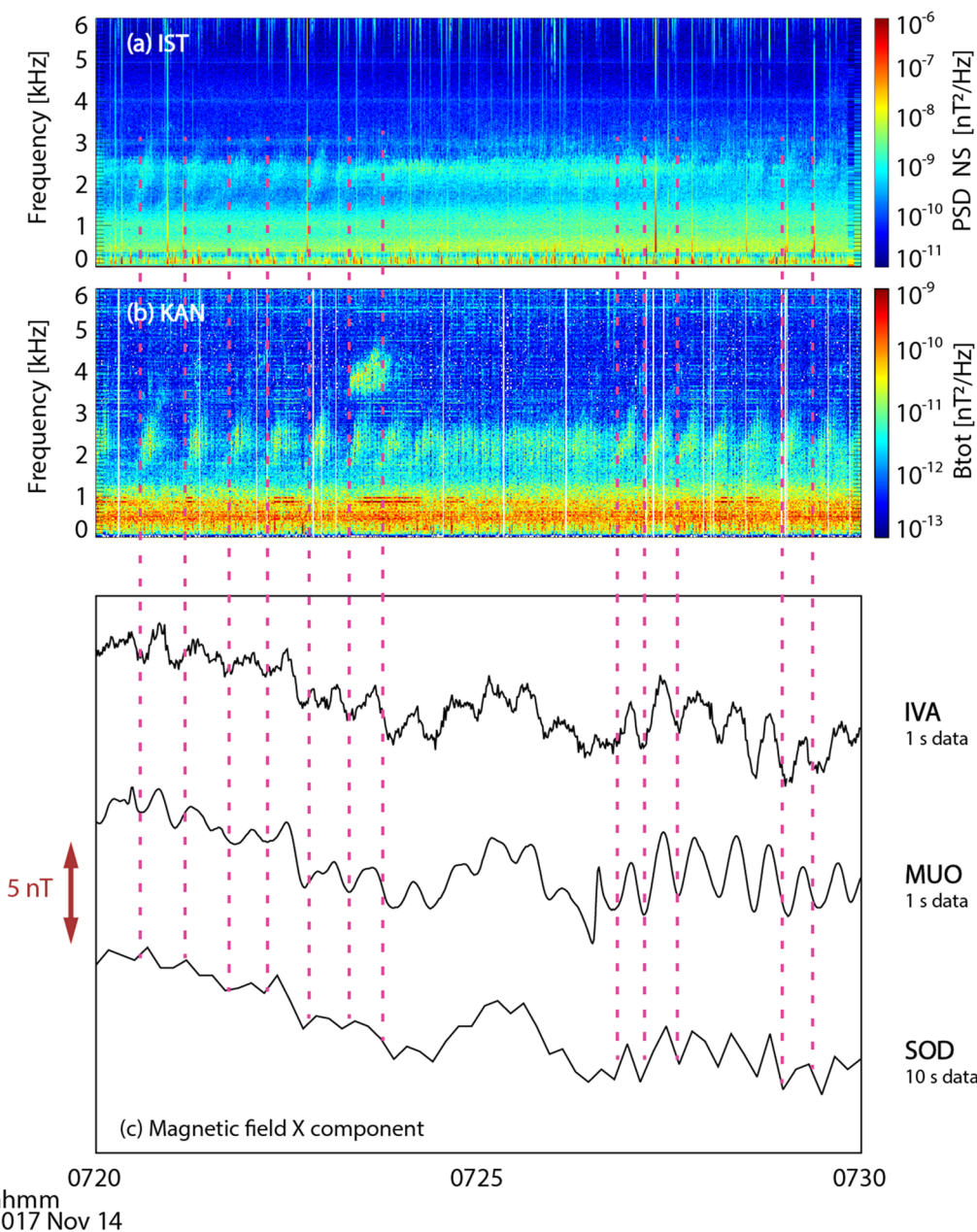
Fig. 5 10-min plot wave spectra and magnetic field on 14 November 2017. Wave spectra at **a** IST and **b** KAN showing a 'same QP' event on 14 November 2017 from 07:20 to 07:30 UT. Panel **c** shows the variations of the X component of the magnetic field detected by magnetometers at IVA, MUO, and SOD. Vertical magenta lines indicate the QP elements that correspond with geomagnetic pulsations

could be missing a portion of the QP emissions generated during this period. However, even if the occurrence rate of the waves increases in this period (Martinez-Calderon et al. 2015; Yonezu et al. 2017), the increase of lightning activity and related sferics could also make the detection of the waves more difficult, particularly at stations other than KAN (only station with a functional sferics filter).

Relationship with geomagnetic pulsations

As described in the introduction, QP emissions have been historically classified into two types depending on whether they are observed concurrently with geomagnetic pulsations (type I) or not (type II). In the case of type I emissions, it is believed that compressional ULF magnetic field oscillations modulate the resonant

Martinez-Calderon *et al. Earth, Planets and Space*   (2023) 75:148

Page 11 of 13

conditions of wave growth giving the wave its periodicity. Therefore, we investigated if all the 'same QPs' events were observed with concurrent geomagnetic pulsations or not at the times of simultaneous observations. We use magnetometer data from IVA, MUO, and SOD as they are the closest stations to KAN (Fig. 1).

We found that three of the 'same QPs' events were observed with no geomagnetic pulsations on the ground and are, therefore, easily considered as type II. Another four cases were detected with pulsations of different periodicity to that of the observed QP emissions and thus are also qualified as type II. This was also confirmed by data from the pulsation magnetometer at SOD and IVA. The remaining six events showed limited concurrent pulsations with the QP elements, meaning that they cannot be solely qualified as type I. Figure 5 shows an example of these cases for 14 November 2017 from 07:20 to 07:30 UT. Panels (a) and (b) show the wave spectra at IST and KAN, while panel (c) shows the variations of the X component of the magnetic field at three different magnetometers: IVA, MUO, and SOD. Magenta vertical lines act as guides to show that for some QP elements, the local decrease in the pulsations corresponds to the approximate start of the corresponding QP element. However, this correspondence only lasts for around 40 to 50 min out of a total event duration of 170 min. Therefore, all the remaining six events that show this type of intermittent correspondence between pulsations and QP elements will be classified as mixed type (mix of type I and II).

Some studies have suggested that the pulsations observed on the ground along with the QP waves do not necessarily have to be related to the generation of the QP emission itself. Tixier and Cornilleau-Wehrlin (1986) found that the distinction between types I and II is not as obvious in space observations and even suggested that both types could have the same generation mechanisms. Sato and Matsudo (1986) advanced the hypothesis that the pulsations could be of ionospheric origin, with more recent studies supporting the idea that the pulsation could come from the periodic precipitation of energetic electrons made by the waves themselves (Golkowski et al. 2008; Hayosh et al. 2013). In addition, of course, there is the easier explanation that we are just missing the pulsations on the ground that would be near the generation region in the inner magnetosphere. However, the purpose of this study is not to justify this classification, but just to investigate if all the events observed between KAN and IST had any common characteristics related to pulsations. After all, we found that this was not the case and the longitudinal extent results found in this study are not related to any specific type of QP or the presence of geomagnetic pulsations detected on the ground.

Summary

Using the network of VLF receivers from the PWING network, we focused on the detection of QP emissions at subauroral latitudes and the longitudinal extent of waves showing one-to-one correspondence between multiple stations. We can summarize our findings as follows:

- QP emissions showing the same spectral and temporal features were detected only between two stations, KAN and IST.
- The longitudinal extent of 90% of waves showing one-to-one correspondence at multiple locations was 4 MLT (upper estimate), and even considering lack of data at certain stations, the best-case scenario could not be higher than 7 MLT. We note the very low percentage of waves simultaneously detected at two stations, so we also estimate that most of the time the real extent is lower than 4 MLT.
- The previous point would suggest that the 'same QPs' events likely had a longitudinally extended source region close to 4 MLT.
- We found that these results were independent of the historical QP type definition. Events with one-to-one correspondence at KAN and IST both showed limited correspondence with geomagnetic pulsations and/or total absence of relationship with pulsations on the ground.

Abbreviations

QP	Quasi-periodic
PWING	Study of dynamical variations of Particles and Waves in the INner magnetosphere using ground-based network observations
ATH	Athabasca ground-station (VLF receiver location)
KAN	Kannuslehto ground-station (VLF receiver location)
GAK	Gakona ground-station (VLF receiver location)
HUS	Husafell ground-station (VLF receiver location)
IST	Istok ground-station (VLF receiver location)
KAP	Kapuskasing ground-station (VLF receiver location)
MAI	Maimaga ground-station (VLF receiver location)
NAI	Nain ground-station (VLF receiver location)
ELF	Extremely low-frequency
VLF	Very-low-frequency
MLAT	Magnetic latitude
L	L-shell
kHz	Kilohertz
V	Volts
nT	Nanotesla
UT	Universal time

Martinez-Calderon *et al. Earth, Planets and Space*   (2023) 75:148

Page 12 of 13

Author contributions

TO visually inspected and analyzed the data from all stations and selected relevant cases. CMC supervised TO, revised the data, wrote the manuscript, and made all figures. JM made the original list of QP events detected at KAN for 2017–2018. KS is in charge of the PWING project, JM is the PI of KAN, and AO is the PI of IST. MO made contributions to the design of the VLF network of the PWING project and the interpretation of data. All authors have helped put together the manuscript and given final approval.

Funding

Availability of data and materials

The power spectrum density of VLF data for KAN is publicly available as quick-look plots at https://www.sgo.fi/pub_VLF/. Any additional data in other formats can be requested by contacting the PI of the instrument Jyrki Manninen. Spectral data for ATH, GAK, HUS, IST, MAM, and NAI are available at the ERG data center https://ergsc.isee.nagoya-u.ac.jp/data/ergsc/ground/VLF/. Instrumentation and data analysis at KAN are funded by the Sodankylä Geophysical Observatory and the University of Oulu. Magnetometer data can be found at https://space.fmi.fi/image/plasmon/ for IVA and MUO (1-s data) and at https://space.fmi.fi/image/www/ for SOD (10-s data).

Declarations

Ethics approval and consent to participate
Not applicable.

Consent for publication
Not applicable.

Competing interests
Not applicable.

Author details
[1]Institute for Space-Earth Environmental Research, Nagoya, Japan. [2]Sodankylä Geophysical Observatory, Sodankylä, Finland. [3]ISTP, Russian Academy of Sciences, Irkutsk, Russia. [4]Kanazawa University, Kanazawa, Japan.

References

Barr R, Jones DL, Rodger CJ (2000) ELF and VLF radio waves. J Atmospheric Solar-Terrestrial Phys 62(17-18):1689–1718

Bezděková B, Němec F, Manninen J, Hospodarsky GB, Santolík O, Kurth WS, Hartley DP (2020) Conjugate observations of quasiperiodic emissions by the Van Allen Probes spacecraft and ground-based station Kannuslehto. J Geophys Res Space Phys 125:793. https://doi.org/10.1029/2020JA027793

Golkowski M, Inan US, Gibby AR, Cohen MB (2008) Magnetospheric amplification and emission triggering by ELF/VLF waves injected by the 3.6 MW HAARP ionospheric heater. J Geophys Res Space Phys. https://doi.org/10.1029/2008JA013157

Hayosh M, Pasmanik DL, Demekhov AG, Santolik O, Parrot M, Titova EE (2013) Simultaneous observations of quasi-periodic ELF/VLF wave emissions and electron precipitation by demeter satellite: a case study. J Geophys Res Space Phys 118(7):4523–4533. https://doi.org/10.1002/jgra.50179

Hayosh M, Nemec F, Santolik O, Parrot M (2014) Statistical investigation of VLF quasiperiodic emissions measured by the DEMETER spacecraft. J Geophys Res Space Phys 119(10):8063–8072. https://doi.org/10.1002/2013JA019731

Horne RB, Thorne RM, Shprits YY, Meredith NP, Glauert SA, Smith AJ, Decreau PME (2005) Wave acceleration of electrons in the Van Allen radiation belts. Nature 437(7056):227–230

Kimura I (1974) Interrelation between VLF and ULF emissions. Space Sci Rev 16(3):389–411

Kitamura, T., Jacobs, J., Watanabe, T., & Flint, R. (1968). Investigation of quasiperiodic VLF emissions and their relation to geomagnetic micropulsations.

Manninen, J. (2005). Some aspects of ELF-VLF emissions in geophysical research (Doctoral dissertation). http://www.sgo.fi/Publications/SGO/thesis/ManninenJyrki.pdf

Manninen J, Kleimenova N, Kozyreva O, Bespalov P, Kozlovsky A (2013) Nontypical ground-based quasi-periodic VLF emissions observed at l 5.3 under quiet geomagnetic conditions at night. J Atmos Solar Terr Phys 99:123–128

Manninen J, Demekhov A, Titova E, Kozlovsky A, Pasmanik D (2014) Quasiperiodic VLF emissions with short-period modulation and their relationship to whistlers: a case study. J Geophys Res Space Phys 119(5):3544–3557

Martinez-Calderon, C. (2016). Study of magnetospheric ELF/VLF waves at subauroral latitudes using ground-base and spacecraft observations (Doctoral dissertation). Graduate School of Science (SSe), Nagoya University.

Martinez-Calderon C, Shiokawa K, Miyoshi Y, Ozaki M, Schofield I, Connors M (2015) Statistical study of ELF/VLF emissions at subauroral latitudes in Athabasca, Canada. J Geophys Res Space Phys 120:8455–8469. https://doi.org/10.1002/2015JA021347

Martinez-Calderon C, Nemec F, Katoh Y, Shiokawa K, Kletzing C, Hospodarsky G et al (2020) Spatial extent of quasiperiodic emissions simultaneously observed by Arase and Van Allen probes on 29 November 2018. J Geophys Res Space Phys 125(9):e2020JA028126

Martinez-Calderon C, Katoh Y, Manninen J, Santolik O, Kasahara Y, Matsuda S et al (2021) Multievent study of characteristics and propagation of naturally occurring ELF/VLF waves using high-latitude ground observations and conjunctions with the Arase satellite. J Geophys Res Space Phys 126:e2020JA028682. https://doi.org/10.1029/2020JA028682

Meredith NP, Horne RB, Thorne RM, Anderson RR (2003) Favored regions for chorus-driven electron acceleration to relativistic energies in the earth's outer radiation belt. Geophys Res Lett 30(16):408. https://doi.org/10.1029/2003GL017698

Nemec F, Santolık O, Parrot M, Pickett J, Hayosh M, Cornilleau-Wehrlin N (2013a) Conjugate observations of quasi-periodic emissions by CLUSTER and DEMETER spacecraft. J Geophys Res Space Phys 118(1):198–208

Nemec F, Santolık O, Pickett J, Parrot M, Cornilleau-Wehrlin N (2013b) Quasiperiodic emissions observed by the cluster spacecraft and their association with ULF magnetic pulsations. J Geophys Res Space Phys 118(7):4210–4220

Nemec F, Hospodarsky G, Bezdekova B, Demekhov A, Pasmanik D, Santolık O, Hartley D (2018) Quasiperiodic whistler mode emissions observed by the Van Allen probes spacecraft. J Geophys Res Space Phys 123(11):8969–8982

Ozaki M, Yagitani S, Nagano I, Hata Y, Yamagishi H, Sato N, Kadokura A (2008a) Localization of VLF ionospheric exit point by comparison of multipoint ground-based observation with full-wave analysis. Polar Sci 2(4):237–249

Ozaki M, Yagitani S, Nagano I, Kasahara Y, Yamagishi H, Sato N, Kadokura A (2010) Simultaneous ground-based and satellite observations of natural VLF waves in Antarctica: a case study of downward ionospheric penetration of whistler-mode waves. Polar Scie. https://doi.org/10.1016/j.polar.2010.04.008

Parrot M, Santolík O, Cornilleau-Wehrlin N, Maksimovic M, Harvey C (2003) Magnetospherically reflected chorus waves revealed by ray tracing with CLUSTER data. Ann Geophys 21:1111–1120

Santolík O, Chum J, Parrot M, Gurnett DA, Pickett JS, Cornilleau-Wehrlin N (2006) Propagation of whistler mode chorus to low altitudes: spacecraft

observations of structured ELF hiss. J Geophys Res 111:A10208. https://doi.org/10.1029/2005JA011462

Santolík O, Parrot M, Němec F (2016) Propagation of equatorial noise to low altitudes: decoupling from the magnetosonic mode. Geophys Res Lett 43:6694–6704. https://doi.org/10.1002/2016GL069582

Sato N, Fukunishi H (1981) Interaction between ELF-VLF emissions and magnetic pulsations: classification of quasi-periodic ELF-VLF emissions based on frequency time spectra. J Geophys Res Space Physics 86(A1):19–29

Sato N, Matsudo T (1986) Origin of magnetic pulsations associated with regular period VLF pulsations (type 2 QP) observed on the ground at Syowa station. J Geophys Res Space Phys 91(A10):11179–11185

Sato N, Hayashi K, Kokubun S, Oguti T, Fukunishi H (1974) Relation ships between quasi-periodic VLF emission and geomagnetic pulsation. J Atmos Terr Phys 36(9):1515–1526

Shiokawa K, Katoh Y, Hamaguchi Y, Yamamoto Y, Adachi T, Ozaki M et al (2017) Ground-based instruments of the PWING project to investigate dynamics of the inner magnetosphere at subauroral latitudes as a part of the ERG-ground coordinated observation network. Earth Planet Space 69(1):1–21. https://doi.org/10.1186/s40623-017-0745-9

Takeshita Y, Shiokawa K, Ozaki M, Manninen J, Oyama S-I, Connors M, Oinats A (2019) Longitudinal extent of magnetospheric ELF/VLF waves using multipoint PWING ground stations at subauroral latitudes. J Geophys Res Space Phys 124(12):9881–9892

Takeshita Y, Shiokawa K, Miyoshi Y, Ozaki M, Kasahara Y, Oyama S, Kurkin V (2020) Study of spatiotemporal development of global distribution of magnetospheric ELF/VLF waves using ground-based and satellite observations, and RAM-SCB simulations, for the march and november 2017 storms. J Geophys Res Space Phys. https://doi.org/10.1029/2020JA028216

Tanskanen E (2009) A comprehensive high-throughput analysis of substorms observed by image magnetometer network: years 1993–2003 examined. J Geophys Res Space Phys. https://doi.org/10.1029/2008JA013682

Thorne RM (2010) Radiation belt dynamics: the importance of wave-particle interactions. Geophys Res Lett. https://doi.org/10.1029/2010GL044990

Titova E, Kozelov B, Demekhov A, Manninen J, Santolik O, Kletzing C, Reeves G (2015) Identification of the source of quasiperiodic VLF emissions using ground-based and Van Allen probes satellite observations. Geophys Res Lett. https://doi.org/10.1002/2015GL064911

Tixier M, Cornilleau-Wehrlin N (1986) How are the VLF quasi-periodic emissions controlled by harmonics of field line oscillations? The results of a comparison between ground and geos satellites measurements. J Geophys Res Space Physics 91(A6):6899–6919. https://doi.org/10.1029/JA091iA06p06899

Trakhtengerts VY, Rycroft MJ (2008) Whistler and alfven mode cyclotron masers in space. Cambridge University Press Cambridge, Cambridge

Yonezu Y, Shiokawa K, Connors M, Ozaki M, Manninen JK, Yamagishi H, Okada M (2017) Simultaneous observations of magnetospheric ELF/VLF emissions in Canada, Finland, and Antarctica. J Geophys Res Space Phys. https://doi.org/10.1002/2017JA024211

Publisher's Note